NANO LETTERS

LETTER

pubs.acs.org/NanoLett

Incident-Angle-Modulated Molecular Plasmonic Switches: A Case of Weak Exciton−Plasmon Coupling

Yue Bing Zheng,[†,§] Brian Kiraly,[†] Sarawut Cheunkar,[‡] Tony Jun Huang,[*,†] and Paul S. Weiss[*,§]

[†]Department of Engineering Science and Mechanics and [‡]Department of Chemistry, The Pennsylvania State University, University Park, Pennsylvania 16802, United States

[§]California NanoSystems Institute and Departments of Chemistry & Biochemistry and Materials Science & Engineering, University of California, Los Angeles, Los Angeles, California 90095, United States

ABSTRACT: We have designed an angularly tunable plasmonic system that consists of Au nanodisks in combination with molecules of photoswitchable resonance, spiropyran, to gain new insights into weak exciton−plasmon couplings. In the weak exciton−plasmon coupling regime, switching molecular resonance can induce localized surface plasmon resonance (LSPR) peak shifts due to the change in the refractive index of the molecular materials. On the basis of the angle-resolved spectroscopic study of the nanodisk−spiropyran system both with and without UV irradiation, we reveal an unusual "zigzag" curve for the LSPR peak shifts (due to the photoswitching of the molecular resonance) as a function of the original LSPR peak wavelength. A further theoretical analysis attributes the "zigzag" curve to two significant competing effects that depend on the incident angle of the probe light: plasmon-enhanced molecular resonance absorption and LSPR sensitivity to the surroundings' refractive index.

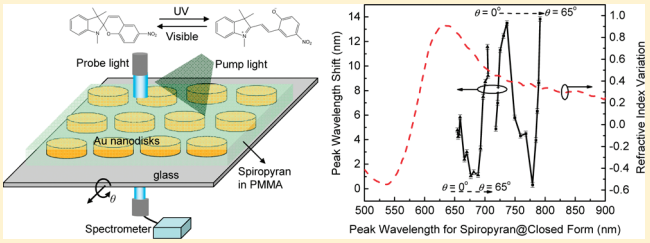

KEYWORDS: Plasmon, molecular switch, exciton-plasmon coupling, molecular plasmonics, active plasmonics

Metal nanoparticles functionalized with molecules of switchable resonances are emerging as functional materials for ultrasmall and energy-saving active nanophotonic devices.[1−4] In these devices, switching of molecular resonances is transduced into active control of the localized surface plasmon resonance (LSPR) of metal nanoparticles by modifying the interactions between the metal nanoparticles and molecules.[5−12] Among the most notable interactions are exciton−plasmon couplings.[13−26] Switching molecules from resonance to nonresonance leads to switching of the exciton−plasmon couplings from "on" to "off" or vice versa.[5] The switching of the couplings is responsible for the modulation of the LSPR, including peak wavelength shifts, peak intensity change, and band shape change.[5,8,27,28] Therefore, understanding of the exciton−plasmon couplings and the effects of their switching on the LSPR is important for the optimal operation of the devices.

Two types of exciton−plasmon coupling—strong coupling and weak coupling—exist in the resonant molecule−metal nanoparticle complexes. Strong exciton−plasmon coupling leads to Rabi splitting due to the formation of exciton−plasmon hybridized states, where a single LSPR band develops into two or more bands.[13−15] Therefore, switching "on" or "off" the strong couplings by controlling the molecular resonance can lead to the "appearance" or "disappearance" of the splitting of the LSPR band, respectively. Recently, experimental demonstration of the strong-coupling switching has been reported by Wang and co-workers.[5] In the weak-coupling regime, the resonant molecules can be treated as dielectric materials with a complex refractive index (RI) in dispersion. Through the Kramers−Kronig relations, the wavelength dependence of the real part of the RI is related to the molecular absorption resonance as described by the imaginary part of the RI.[29] As a result, switching the molecular resonance can change the real part of the RI and thus cause LSPR peak shifts due to the sensitivity of the LSPR to the refractive index of the surroundings. Van Duyne and co-workers reported weak exciton−plasmon coupling but with molecules of nonswitchable resonance.[29] In this Letter, we report weak exciton−plasmon coupling between molecules of photoswitchable resonance and metal nanoparticles. Furthermore, we have developed an angularly tunable plasmonic system to study the couplings using only a single sample; the new phenomena of incident-angle-modulated exciton−plasmon coupling processes are observed and explained.

The main component of the angular-tunable plasmonic system consists of coupled Au nanodisk arrays (Figure 1a). Figure 1b is a representative scanning electron microscopy (SEM) image of a Au nanodisk array on a glass substrate. Due to modifications in both far- and near-field coupling among the nanodisks, the arrays exhibit a continuous LSPR red shift when the incident angle of light is increased from normal (0°) to 65°.[15] The real-time tunable LSPR enables us to use a single sample to cover a broad range of LSPR wavelengths that facilitates the measurements of the LSPR shift at different wavelengths. This single-sample strategy helps avoid the use of many samples with various LSPR responses and any potential inconsistent experimental conditions due to sample

Received: February 13, 2011
Revised: April 12, 2011
Published: April 18, 2011

deviation in topology, geometry, or molecular distribution. Therefore, it is a highly reliable method to compare LSPR data before and after switching and to draw solid conclusions on the effects of molecular switching on the modulation of LSPR.

We chose the molecular switch, spiropyran (1′,3′,-dihydro-1′,3′,3′-trimethyl-6-nitrospiro[2*H*-1-benzopyran-2,2′-(2*H*)-indole]) (Figure 2a), for its photoswitchable, high-intensity, and broad-bandwidth molecular resonance.[30] Photoirradiation of spiropyran with UV (350 nm) pump light transforms the molecule from its closed form to its open form, associated with the appearance of a broad-bandwidth molecular resonance centered at a wavelength of 580 nm (Figure 2b). By photoswitching this broad-bandwidth molecular resonance, we can induce a refractive-index change in the molecular materials within a wide range of wavelengths because of the Kramers−Kronig relations (Figure 2b). This wide range of wavelengths enables us to detune the LSPR of the metal nanoparticles from the resonant peak of the molecules within the limit of the wavelength range of the refractive index variation. By detuning the two resonances, we can avoid strong exciton−plasmon coupling and thus focus on the weak-coupling regime.

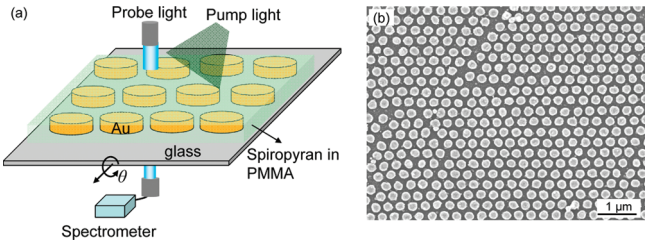

Figure 1. (a) Schematic of the sample consisting of a Au nanodisk array sandwiched between a glass substrate and a thin PMMA film mixed with the spiropyran, and the experimental setup for the angle-resolved spectrum measurements. (b) A representative scanning electron micrograph of a Au nanodisk array on a glass substrate.

Figure 1a shows a schematic of the sample structure and the experimental setup for the angle-resolved spectral measurements. The sample consists of a Au nanodisk array sandwiched between a glass substrate and a poly(methyl methacrylate) (PMMA) thin film mixed with spiropyran molecules. While recording the absorption spectra using a spectrometer (USB4000, Ocean Optics Inc., Dunedin, Florida, USA), we continuously rotated the sample along the out-of-plane direction to vary the incident angle of the probe light (θ) from 0° to 65° at intervals of 5°. The UV pump light, which is used to switch the spiropyran from its closed form to its open form, is directed onto the sample at a certain angle. The hexagonal arrays of Au nanodisks of different sizes were fabricated on glass substrates with nanosphere lithography.[31] The spiropyran was purchased from

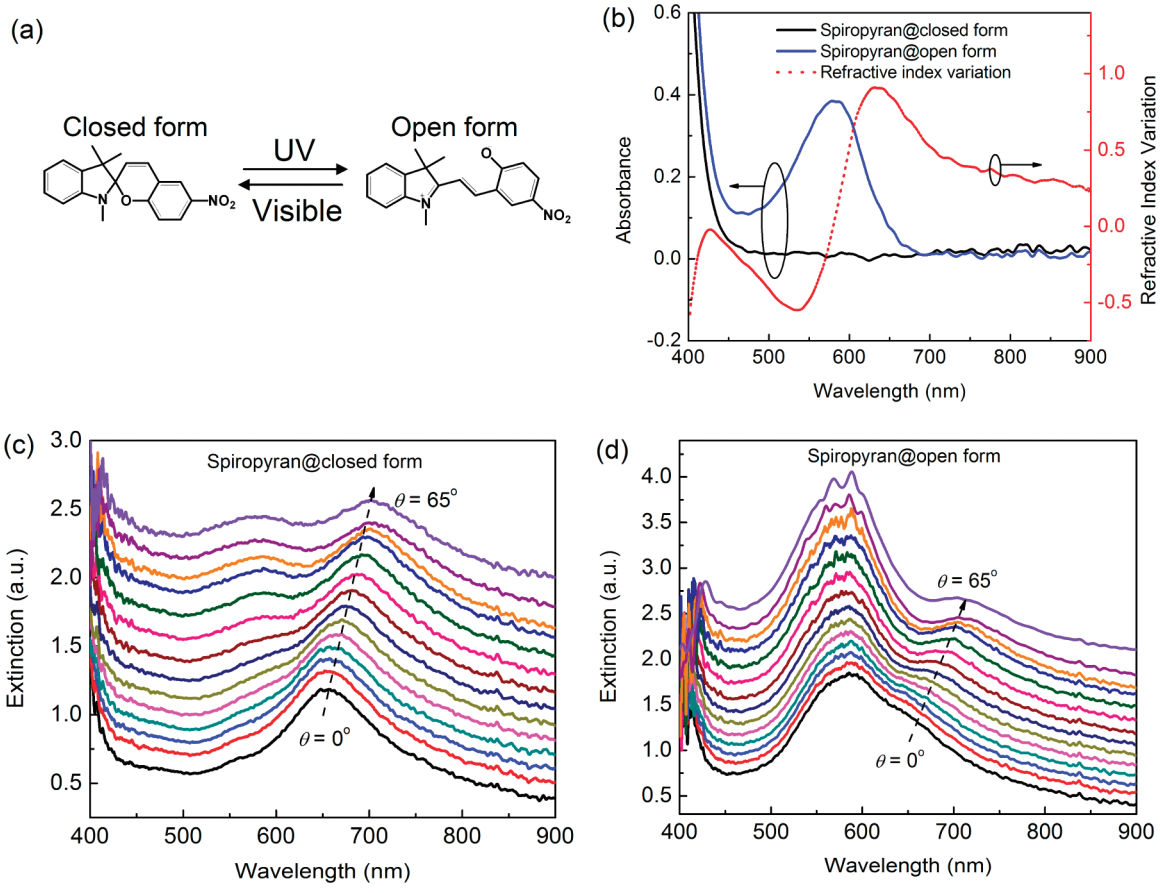

Figure 2. (a) Structure of the spiropyran in closed (without UV) and open (with UV) forms. (b) Absorbance spectra of a spiropyran-mixed PMMA thin film on a glass substrate without (back line) and with (blue line) UV irradiation, and the change in the refractive index dispersion (dotted red line) induced by the photoisomerization of the spiropyran as calculated by the Kramers−Kronig relations. (c) A sequence of angle-resolved extinction spectra from the sandwiched sample with spiropyran in its closed form. (d) A sequence of angle-resolved extinction spectra from the sandwiched sample with spiropyran in its open form. In (c) and (d), the dashed arrows indicate the evolution of the in-plane dipole resonance of the Au nanodisk array, and the incident angle θ is changed from 0° to 65° at intervals of 5°.

dx.doi.org/10.1021/nl200524b |*Nano Lett.* 2011, 11, 2061–2065

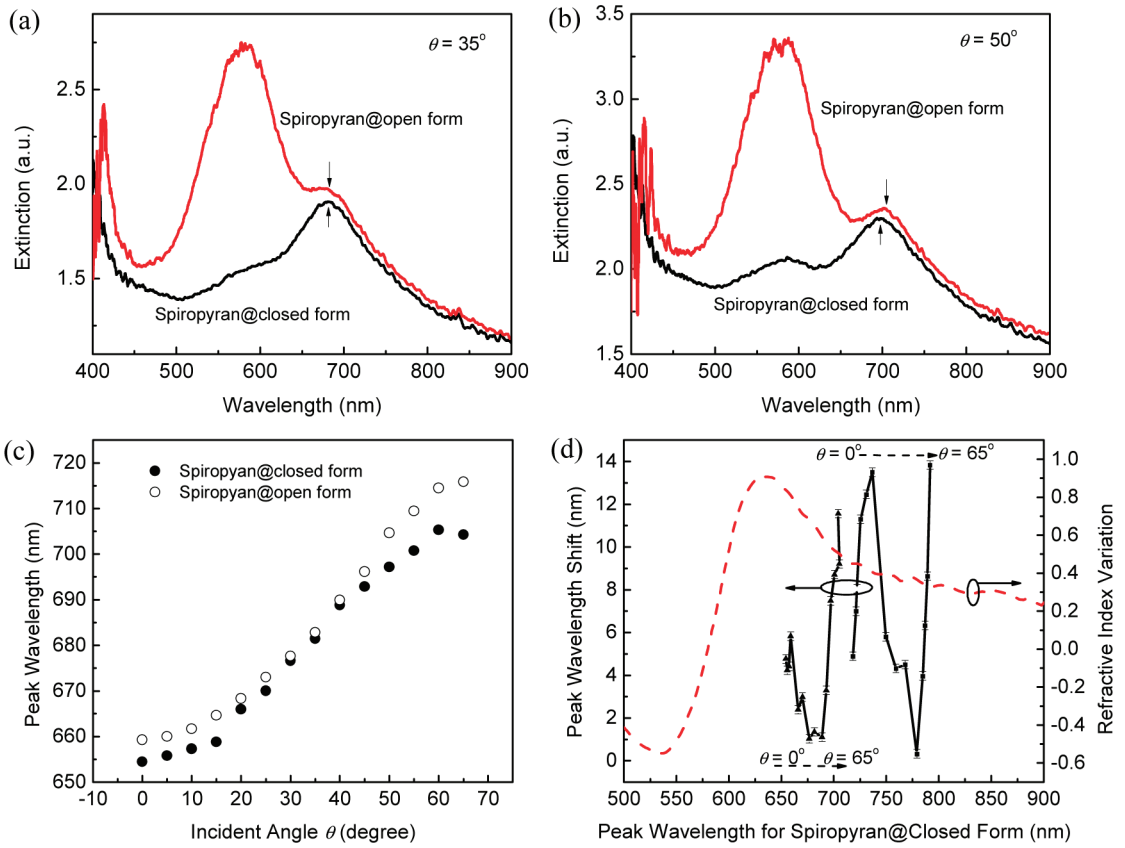

Figure 3. (a) The extinction spectra of the sandwiched sample with the spiropyran in its closed form (black line) and open form (red line), respectively, recorded at an incident angle $\theta = 35°$. (b) The extinction spectra of the sandwiched sample with the spiropyran in its closed form (black line) and open form (red line), respectively, taken at an incident angle $\theta = 50°$. In (a) and (b), the arrows indicate the peaks of the in-plane LSPR and the strong band centered at a wavelength of 580 nm reveals the resonant absorption of the spiropryan in its open form. (c) The peak wavelengths of the in-plane LSPR as a function of incident angle θ with the spiropyran in its closed and open forms, respectively, according to panels c and d of Figure 2. (d) The dispersion curve of the peak wavelength shift as a function of the peak wavelength of the LSPR with the spiropyran in its closed form for the two different sandwiched samples. The curve for the refractive index variation from Figure 2b is also shown here.

Aldrich and prepared in a 2 wt % PMMA solution with a spiropyran to PMMA weight ratio of 1:1. The mixture was spin-coated onto the substrates with Au nanodisk arrays, with the resulting thin films having a thickness of ~1 μm. The molecular formula and absorption spectra of the closed and open forms (upon UV irradiation) of the spiropyran are shown in Figure 2a and Figure 2b, respectively. Measurements were carried out on the mixed PMMA thin films on glass substrates. Upon UV irradiation of the sample, the spiropyran switched from its closed form to its open form, resulting in the appearance of a resonant absorption band centered at a wavelength of 580 nm (Figure 2b). Using the Kramers−Kronig relations, we transformed the two absorption spectra into the wavelength-dependent change in refractive index (Δn) of the molecular materials. As shown in Figure 2b, a large range of wavelengths having nonzero Δn is associated with the appearance of the resonant band due to photoisomerization (upon UV irradiation) of spiropyran.

Figure 2c shows a sequence of angle-resolved extinction spectra from the sandwiched sample with the spiropyran in the closed form (before UV irradiation). At normal incidence ($\theta = 0°$), a single strong in-plane LSPR was found at a wavelength of 654.5 nm. As the incident angle was changed from 0° to 65°, the peak wavelength continuously red-shifted to 704.3 nm. An additional absorption band appeared in the spectra in the range from 500 to 600 nm when the incident angle was increased. This additional band arose from the out-of-plane LSPR.[32] Figure 2d shows a sequence of angle-resolved extinction spectra from the sandwiched sample with the spiropyran in open form (upon UV irradiation). At normal incidence ($\theta = 0°$), the in-plane LSPR shifted from 654.5 nm (before UV irradiation as shown in Figure 2c) to 659.3 nm due to UV-induced photoisomerization of the spiropryan molecules. As the incident angle was changed from 0° to 65°, the peak wavelength continuously red-shifted to 715.8 nm. The strong band centered at 580 nm in the extinction spectra of Figure 2d is the same as that in the Figure 2b and is due to the resonant absorption of the photoisomerized spiropryan molecules in the PMMA thin film. In the spectral analysis, the molecular absorption band was subtracted as background from the system extinction in Figure 2d to get an accurate measurement of the LSPR wavelength.

Panels a and b of Figure 3 make a direct comparison of the extinction spectra of the sample with and without UV irradiation measured at $\theta = 35°$ and $\theta = 50°$, respectively. At $\theta = 35°$, the in-plane LSPR red-shifted from 681.5 to 682.8 nm after UV irradiation; at $\theta = 50°$, the UV irradiation in-plane LSPR red-shifted from 697.2 to 704.7 nm. Both red shifts agree with the refractive index variation induced by photoisomerization of the spiropyran molecules (Figure 2b). From the dispersion curve in Figure 2b, we can see that the refractive index increased (i.e., a positive refractive index variation) at wavelengths of 681.5 and 697.2 nm due to the

dx.doi.org/10.1021/nl200524b |Nano Lett. 2011, 11, 2061–2065

photoisomerization process. An increased refractive index always results in a red shift of a LSPR. The LSPR peak wavelengths with and without UV irradiation as a function of θ are given in Figure 3c.

To gain more insight into how the incident angle modulates the molecular-switching-induced peak shift of the LSPR, we plotted the peak wavelength shift of the LSPR as a function of its peak wavelength without UV irradiation in Figure 3d. The dispersion curve from Figure 2b is also shown in Figure 3d. Two samples, whose LSPR fall into distinct spectral ranges, were studied. Each sample contains 14 data points corresponding to incident angles scanned from 0° to 65° (indicated by the dashed arrows in Figure 3d). In each sample, the photoisomerization-induced peak shift in the angle-resolved spectra "zigzags" as a function of the initial LSPR peak wavelengths instead of following the refractive index dispersion. The inconsistency between the LSPR peak shift and refractive index dispersion can be attributed primarily to two plasmon-based phenomena responsive to the incident angle of light. The first is based on the plasmon-enhanced absorption of molecules near metal nanostructures.[29,30,33,34] According to the Kramers−Kronig relations, enhanced absorption corresponds to an increase in the refractive index dispersion and thus a larger LSPR peak shift. The absorption enhancement of the spiropyran is subject to change as a function of the incident angle θ, because the in-plane LSPR that contributes to the enhanced absorption is reduced when the incident angle θ is increased. This is confirmed by the decreased intensity and broadened bandwidth of the LSPR when θ is increased (Figure 2c). As a result of the change in the enhanced absorption, the change in refractive index deviates from the dispersion curve in Figure 2b. Meanwhile, the peak wavelength of the LSPR independently red shifts as θ increases. It has been shown that LSPR at longer wavelengths have higher sensitivity to changes in the refractive index;[31,35,36] therefore, the sensitivity increases as θ increases. The "zigzag" LSPR peak shift that appears during molecular switching is a result of the combined effects of the decreased molecular absorption enhancement and the increased LSPR sensitivity when the incident angle of probe light is increased from 0° to 65°. Specifically, the increase in LSPR sensitivity dominates over the decrease in molecular absorption enhancement in the ranges of the lowest and highest incident angles, which leads to the increased LSPR peak shifts when θ is increased. The decrease in molecular absorption enhancement dominates in the intermediate range of the incident angle, which leads to the deceased LSPR peak shifts when θ is increased. In addition, overlap of the molecular resonance and out-of-plane LSPR at incident angles above 40° (Figure 2c) will induce strong exciton−plasmon coupling, which produces hybridized states.[13,14] One of the hybridized states would have a largely red-shifted resonance that could overlap with the in-plane LSPR, possibly also accounting for the increased red shift of the in-plane LSPR at the highest incident angles.

In summary, we have designed a tunable LSPR system to investigate weak coupling between plasmon and switchable molecular resonances. By varying the incident angle of light, we succeed in tuning the far- and near-field electromagnetic couplings between Au nanodisks in hexagonal arrays to shift the LSPR peak wavelength continuously. The photoswitchable spiropyran is used due to its relatively broad-bandwidth resonance and thus the switching-induced change in the refractive index dispersion over a wide wavelength range. An interesting "zigzag" curve is obtained for the LSPR peak shifts as a function of the initial LSPR peak wavelength. In contrast to the refractive index dispersion, this dependence is attributed primarily to two combined effects from the plasmon-enhanced molecular absorption and the LSPR sensitivity to the change in the refractive index of the surroundings. Both of the effects are modulated by the incident angle of the probe light in our study. The tunable plasmonic system serves as a new platform for exploring the rich physics behind the interactions between metal nanoparticles and molecular switches. It also offers opportunities for exploiting these switchable interactions in the development of novel active plasmonic devices.[37−46]

AUTHOR INFORMATION

Corresponding Author

*E-mail: Tony Jun Huang, junhuang@psu.edu; Paul S. Weiss, psw@cnsi.ucla.edu.

ACKNOWLEDGMENT

We thank the NSF-supported Center for Nanoscale Science (MRSEC), the Department of Energy (Grant Nos. DE-SC00-05161 and DE-FG02-07ER15877), the Air Force Office of Scientific Research (FA9550-08-1-0349), the National Science Foundation (ECCS-0801922, ECCS-0609128, and ECCS-0609128), and the Kavli Foundation for support of the work described here.

REFERENCES

(1) Klajn, R.; Stoddart, J. F.; Grzybowski, B. A. *Chem. Soc. Rev.* **2010**, *39*, 2203.
(2) Ye, T.; Kumar, A. S.; Saha, S.; Takami, T.; Huang, T. J.; Stoddart, J. F.; Weiss, P. S. *ACS Nano* **2010**, *4*, 3697.
(3) Kumar, A. S.; Ye, T.; Takami, T.; Yu, B.-C.; Flatt, A. K.; Tour, J. M.; Weiss, P. S. *Nano Lett.* **2008**, *8*, 1644.
(4) Browne, W. R.; Feringa, B. L. *Annu. Rev. Phys. Chem.* **2009**, *60*, 407.
(5) Ming, T.; Zhao, L.; Xiao, M.; Wang, J. *Small* **2010**, *6*, 2514.
(6) Chen, H.; Ming, T.; Zhao, L.; Wang, F.; Sun, L.-D.; Wang, J.; Yan, C.-H. *Nano Today* **2010**, *5*, 494.
(7) Zheng, Y. B.; Yang, Y. W.; Jensen, L.; Fang, L.; Juluri, B. K.; Flood, A. H.; Weiss, P. S.; Stoddart, J. F.; Huang, T. J. *Nano Lett.* **2009**, *9*, 819.
(8) Zhao, J.; Das, A.; Zhang, X.; Schatz, G. C.; Sligar, S. G.; Van Duyne, R. P. *J. Am. Chem. Soc.* **2006**, *128*, 11004.
(9) Liu, G. L.; Long, Y. T.; Choi, Y.; Kang, T.; Lee, L. P. *Nat. Methods* **2007**, *4*, 1015.
(10) Nishi, H.; Asahi, T.; Kobatake, S. *J. Phys. Chem. C* **2009**, *113*, 17359.
(11) van der Molen, S. J.; Liao, J.; Kudernac, T.; Agustsson, J. S.; Bernard, L.; Calame, M.; van Wees, B. J.; Feringa, B. L.; Schönenberger, C. *Nano Lett.* **2008**, *9*, 76.
(12) Dintinger, J.; Robel, I.; Kamat, P. V.; Genet, C.; Ebbesen, T. W. *Adv. Mater.* **2006**, *18*, 1645.
(13) Fofang, N. T.; Park, T. H.; Neumann, O.; Mirin, N. A.; Nordlander, P.; Halas, N. J. *Nano Lett.* **2008**, *8*, 3481.
(14) Wurtz, G. A.; Evans, P. R.; Hendren, W.; Atkinson, R.; Dickson, W.; Pollard, R. J.; Zayats, A. V.; Harrison, W.; Bower, C. *Nano Lett.* **2007**, *7*, 1297.
(15) Zheng, Y. B.; Juluri, B. K.; Jensen, L. L.; Amed, D.; Lu, M.; Jensen, L.; Huang, T. J. *Adv. Mater.* **2010**, *22*, 3603.
(16) Lee, J.; Hernandez, P.; Govorov, A. O.; Kotov, N. A. *Nat. Mater.* **2007**, *6*, 291.
(17) Sugawara, Y.; Kelf, T. A.; Baumberg, J. J.; Abdelsalam, M. E.; Bartlett, P. N. *Phys. Rev. Lett.* **2006**, *97*, 266808.
(18) Juluri, B. K.; Lu, M. Q.; Zheng, Y. B.; Huang, T. J.; Jensen, L. *J. Phys. Chem. C* **2009**, *113*, 18499.

(19) Savasta, S.; Saija, R.; Ridolfo, A.; Di Stefano, O.; Denti, P.; Borghese, F. *ACS Nano* **2010**, *4*, 6369.
(20) Ni, W.; Chen, H.; Su, J.; Sun, Z.; Wang, J.; Wu, H. *J. Am. Chem. Soc.* **2010**, *132*, 4806.
(21) Ni, W.; Yang, Z.; Chen, H.; Li, L.; Wang, J. *J. Am. Chem. Soc.* **2008**, *130*, 6692.
(22) Ni, W.; Ambjörnsson, T.; Apell, S. P.; Chen, H.; Wang, J. *Nano Lett.* **2009**, *10*, 77.
(23) Witlicki, E. H.; Andersen, S. S.; Hansen, S. W.; Jeppesen, J. O.; Wong, E. W.; Jensen, L.; Flood, A. H. *J. Am. Chem. Soc.* **2010**, *132*, 6099.
(24) Achermann, M. *J. Phys. Chem. Lett.* **2010**, *1*, 2837.
(25) Vasa, P.; Lienau, C. *Angew. Chem., Int. Ed.* **2010**, *49*, 2476.
(26) Salomon, A.; Genet, C.; Ebbesen, T. W. *Angew. Chem., Int. Ed.* **2009**, *48*, 8748.
(27) Zhao, J.; Jensen, L.; Sung, J. H.; Zou, S. L.; Schatz, G. C.; Van Duyne, R. P. *J. Am. Chem. Soc.* **2007**, *129*, 7647.
(28) Mayer, K. M.; Lee, S.; Liao, H.; Rostro, B. C.; Fuentes, A.; Scully, P. T.; Nehl, C. L.; Hafner, J. H. *ACS Nano* **2008**, *2*, 687.
(29) Haes, A. J.; Zou, S. L.; Zhao, J.; Schatz, G. C.; Van Duyne, R. P. *J. Am. Chem. Soc.* **2006**, *128*, 10905.
(30) Dintinger, J.; Klein, S.; Ebbesen, T. W. *Adv. Mater.* **2006**, *18*, 1267.
(31) Zheng, Y. B.; Juluri, B. K.; Mao, X. L.; Walker, T. R.; Huang, T. J. *J. Appl. Phys.* **2008**, *103*, 014308.
(32) Chaturvedi, P.; Hsu, K. H.; Kumar, A.; Fung, K. H.; Mabon, J. C.; Fang, N. X. *ACS Nano* **2009**, *3*, 2965.
(33) Pala, R. A.; Shimizu, K. T.; Melosh, N. A.; Brongersma, M. L. *Nano Lett.* **2008**, *8*, 1506.
(34) Pacifici, D.; Lezec, H. J.; Atwater, H. A. *Nat. Photonics* **2007**, *1*, 402.
(35) Gao, H.; Yang, J.-C.; Lin, J. Y.; Stuparu, A. D.; Lee, M. H.; Mrksich, M.; Odom, T. W. *Nano Lett.* **2010**, *10*, 2549.
(36) Bukasov, R.; Shumaker-Parry, J. S. *Nano Lett.* **2007**, *7*, 1113.
(37) Leroux, Y.; Lacroix, J. C.; Fave, C.; Stockhausen, V.; Felidj, N.; Grand, J.; Hohenau, A.; Krenn, J. R. *Nano Lett.* **2009**, *9*, 2144.
(38) MacDonald, K. F.; Zheludev, N. I. *Laser Photonics Rev.* **2010**, *4*, 562.
(39) Chen, H. T.; Padilla, W. J.; Zide, J. M. O.; Gossard, A. C.; Taylor, A. J.; Averitt, R. D. *Nature* **2006**, *444*, 597.
(40) MacDonald, K. F.; Samson, Z. L.; Stockman, M. I.; Zheludev, N. I. *Nat. Photonics* **2009**, *3*, 55.
(41) Maier, S. A.; Brongersma, M. L.; Kik, P. G.; Meltzer, S.; Requicha, A. A. G.; Atwater, H. A. *Adv. Mater.* **2001**, *13*, 1501.
(42) Sönnichsen, C.; Reinhard, B. M.; Liphardt, J.; Alivisatos, A. P. *Nat. Biotechnol.* **2005**, *23*, 741.
(43) Stockhausen, V.; Martin, P.; Ghilane, J.; Leroux, Y.; Randriamahazaka, H.; Grand, J.; Felidj, N.; Lacroix, J. C. *J. Am. Chem. Soc.* **2010**, *132*, 10224.
(44) Dickson, W.; Wurtz, G. A.; Evans, P. R.; Pollard, R. J.; Zayats, A. V. *Nano Lett.* **2008**, *8*, 281.
(45) Hsiao, V. K. S.; Zheng, Y. B.; Juluri, B. K.; Huang, T. J. *Adv. Mater.* **2008**, *20*, 3528.
(46) Oulton, R. F.; Sorger, V. J.; Zentgraf, T.; Ma, R. M.; Gladden, C.; Dai, L.; Bartal, G.; Zhang, X. *Nature* **2009**, *461*, 629.